European Radiology
https://doi.org/10.1007/s00330-019-06368-5

GASTROINTESTINAL

Radiomics analysis using contrast-enhanced CT for preoperative prediction of occult peritoneal metastasis in advanced gastric cancer

Shunli Liu[1] · Jian He[1] · Song Liu[1] · Changfeng Ji[1] · Wenxian Guan[2] · Ling Chen[3] · Yue Guan[4] · Xiaofeng Yang[5] · Zhengyang Zhou[1]

Received: 13 December 2018 / Revised: 23 June 2019 / Accepted: 11 July 2019

Abstract

Objectives To evaluate the predictive value of CT radiomics features derived from the primary tumor in discriminating occult peritoneal metastasis (PM) in advanced gastric cancer (AGC).

Methods Preoperative CT images of 233 patients with AGC were retrospectively analyzed. The region of interest (ROI) was manually drawn along the margin of the lesion on the largest slice of venous CT images, and a total of 539 quantified features were extracted automatically. The intra-class correlation coefficient (ICC) and the absolute correlation coefficient (ACC) were calculated for selecting influential features. A multivariate logistic regression model was constructed based on the training cohort, and the testing cohort validated the reliability of the model. Additionally, another model based on the preoperative clinic-pathological features was also developed. The comparison of the diagnostic performance between the two models was performed using ROC analysis and the Akaike information criterion (AIC) value.

Results Six radiomics features (ID_Energy, LoG(0.5)_Energy, Compactness2, Max Diameter, Orientation, and Surface Area Density) differed significantly between AGCs with and without PM and performed well in distinguishing AGCs with PM from those without PM in the primary cohort (AUC = 0.618–0.658). The radiomics model showed a higher AUC value than each single radiomics feature in the primary cohort (0.741 vs. 0.618–0.658) and similar diagnosis performance in the validation cohort. The radiomics model showed slightly worse diagnostic efficacy than the clinic-pathological model (AUC, 0.724 vs. 0.762).

Conclusion Venous CT radiomics analysis based on the primary tumor provided valuable information for predicting occult PM in AGCs.

Key Points

- *Venous CT radiomics analysis provided valuable information for predicting occult peritoneal metastases in advanced gastric cancer.*
- *CT-based T stage was an independent predictive factor of occult peritoneal metastases in advanced gastric cancer.*
- *A radiomics model showed slightly worse diagnostic efficacy than a clinic-pathological model.*

Keywords Stomach neoplasms · Multidetector computed tomography · Peritoneum · Diagnosis · Neoplasm metastasis

Shunli Liu and Jian He contributed equally to this work.

Electronic supplementary material The online version of this article (https://doi.org/10.1007/s00330-019-06368-5) contains supplementary material, which is available to authorized users.

✉ Xiaofeng Yang
xiaofeng.yang@emory.edu

✉ Zhengyang Zhou
zyzhou@nju.edu.cn

[1] Department of Radiology, Nanjing Drum Tower Hospital, The Affiliated Hospital of Nanjing University Medical School, 321 Zhongshan Road, Nanjing 210008, China

[2] Department of Gastrointestinal Surgery, Nanjing Drum Tower Hospital, The Affiliated Hospital of Nanjing University Medical School, Nanjing 210008, China

[3] Department of Pathology, Nanjing Drum Tower Hospital, The Affiliated Hospital of Nanjing University Medical School, Nanjing 210008, China

[4] School of Electronic Science and Engineering, Nanjing University, Nanjing 210046, China

[5] Department of Radiation Oncology and Winship Cancer Institute, Emory University, Atlanta, GA 30322, USA

Published online: 05 August 2019

Abbreviations

ACC Absolute correlation coefficient
AGC Advanced gastric cancer
AIC Akaike information criterion
AUC Area under the curve
HU Hounsfield unit
ICC Intra-class correlation coefficient
PM Peritoneal metastasis
ROC Receiver operating characteristic
ROI Regions of interest

Introduction

Gastric cancer remains the fifth most common malignancy and the third leading cause of cancer death worldwide [1]. Peritoneal metastasis (PM) is one of the most frequent forms of metastasis in gastric cancer and is generally regarded as an incurable condition with poor prognosis [2, 3]. Therefore, detecting non-invasively PM of gastric cancer prior to surgery would be crucial for avoiding unnecessary resection and selecting optimal therapy in clinical practice.

Currently, staging laparoscopy is the most reliable method to identify clinically occult PM in patients with gastric cancer. NCCN (National Comprehensive Cancer Network) guidelines recommend laparoscopy in T3 and/or N+ stages identified on preoperative imaging. However, laparoscopy is an invasive and costly procedure [4, 5] and is not systematic in clinical practice. CT is the most common tool for preoperative staging in gastric cancer. However, the sensitivity for detecting PM remains low (28–56%) [6–10]. Meanwhile, several studies have reported that MRI, especially DWI, might have a potential to more accurately describe the distribution and extent of peritoneal tumor [11–13]. In general, conventional techniques were not sensitive and accurate enough for detecting peritoneal metastasis preoperatively [14].

Radiomics is a promising tool, converting imaging data into a high-dimensional mineable feature set with a series of data-characterization algorithms. Radiomics explore tumor heterogeneity, pattern, and microenvironment and is promising in assessing and predicting histopathological characteristics, treatment response, clinical outcome, or differential diagnosis in gastric tumors [15–20]. Kim et al reported that preoperative CT texture analysis over the omentum has a potential value for predicting the occult PM of advanced gastric cancers (AGCs) [21]. We formulated the hypothesis that CT radiomics features from the primary tumor might also provide some valuable information for predicting occult PM of AGCs.

This study aimed to evaluate the predictive value of CT radiomics features derived from the primary tumor in discriminating occult PM in AGCs.

Materials and methods

Patients

This retrospective study was approved by the local ethical committee, and the requirement for informed consent was waived.

A total of 468 patients with gastric cancers who underwent surgery at our hospital between January 2014 and December 2017 were identified (Fig. 1).

The inclusion criteria were as follows: (1) a pathological confirmation of gastric carcinomas based on histological examinations of endoscopic-biopsied tissues and (2) availability of contrast-enhanced CT before treatment.

The exclusion criteria were as follows: (1) a history of previous gastric cancer treatment ($n = 37$); (2) no surgical treatment due to definite signs of PM in CT images including omental cake, massive ascites, obvious peritoneum thickening with abnormal enhancement, and discrete nodules away from the primary tumor ($n = 10$) [8, 22]; (3) CT-based T1 staging lesions ($n = 95$) due to a low risk of PM in early-stage gastric cancers [10, 23]; (4) with difficulty of drawing ROIs precisely due to small size (long diameter < 1 cm) ($n = 24$); (5) without a definite margin in CT images ($n = 31$) (seen in Fig. S1); and (6) poor imaging quality due to insufficient distention of the stomach ($n = 32$) or peristaltic motion ($n = 6$).

There were 233 patients (age 24–83 years; median age 64 years) enrolled in our cohort. During surgery, the abdominal and peritoneal conditions were all carefully examined. All suspicious peritoneal implants or ascites were sent for pathological biopsy or cytological examination. The presence of PM was identified using the AJCC (American Joint Committee on Cancer) guidelines in consensus between the pathologists and surgeons. No PM was detected in 188 patients undergoing curative gastrectomy. The remaining 45 patients were diagnosed as occult PM, which is defined as negative PM by preoperative CT but pathologically confirmed PM at laparotomy or laparoscopy [23, 24]. Nine patients underwent palliative surgery, and only laparotomy ($n = 31$) or laparoscopy ($n = 5$) was performed in the remaining patients. Patient and tumor characteristics are summarized in Table 1.

CT image acquisition

CT examinations were performed on a 16- or 64-slice scanner (Light Speed Pro 16, VCT, or Discovery HD 750, GE Healthcare). All patients were requested to fast from food for at least 6 h and received 600–1000 mL water orally to achieve gastric distension prior to the examination. All patients were in the supine position, and the scan covered the upper or the entire abdomen. The patients were trained to hold their breath during CT scanning. Following unenhanced scan,

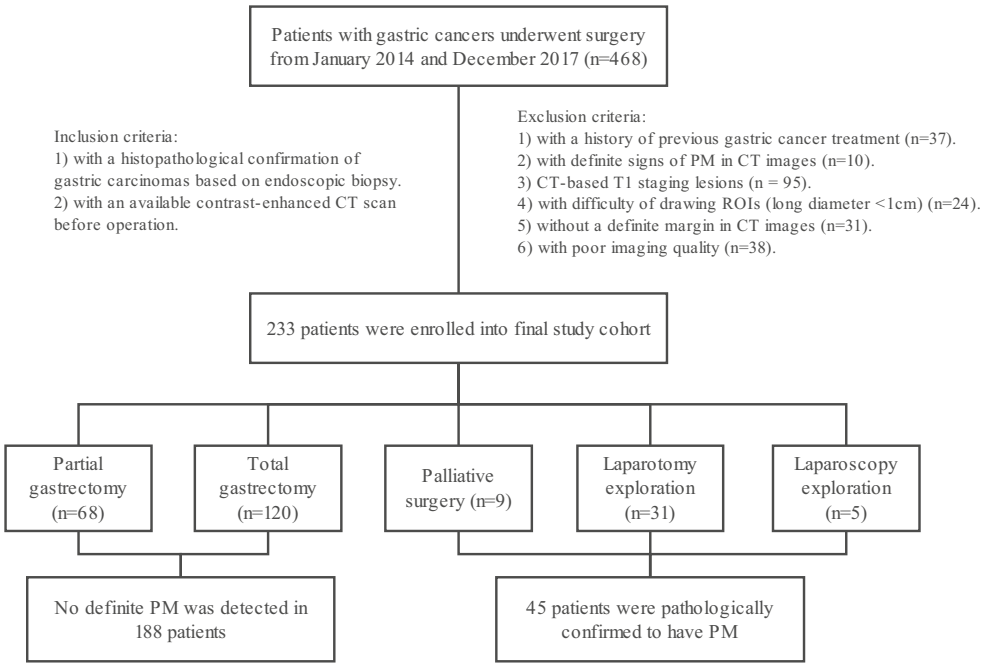

Fig. 1 Flowchart of the patient selection, patient exclusion, and surgical procedures. Data in parentheses are the numbers of patients

Table 1 Univariate analysis of the clinical and pathological characteristics of 233 patients with gastric cancer

Feature	Without PM (%)	With PM (%)	*p* value
No. of patients	188 (80.7)	45 (19.3)	
Gender			0.961
Male	133 (57.1)	32 (13.7)	
Female	55 (23.6)	13 (5.6)	
Age			0.083
< 60 years	58 (24.9)	20 (8.6)	
≥ 60 years	130 (55.8)	25 (10.7)	
Major location			0.002
Cardia	72 (30.9)	5 (2.1)	< 0.001
Body	36 (15.5)	14 (6.0)	0.079
Antrum	80 (34.3)	26 (11.2)	0.065
CT-based T stage			< 0.001
T2/T3	121 (52.0)	11 (4.7)	
T4	67 (28.7)	34 (14.6)	
CT-based N stage			0.136
N0	68 (29.2)	11 (4.7)	
N+	120 (51.5)	34 (14.6)	
Biopsy pathological type			0.019
Adenocarcinoma	147 (63.1)	26 (11.2)	0.005
Signet-ring cell carcinoma	32 (13.7)	15 (6.4)	0.014
Mucinous carcinoma	9 (3.9)	4 (1.7)	0.282
Biopsy differentiation degree			0.018
Poor	97 (41.6)	32 (13.7)	
Moderate/well	91 (39.1)	13 (5.6)	

PM, peritoneal metastasis; *N+*, positive lymph node metastasis

1.5 mL/kg iodinated contrast agent (Omnipaque 350 mg I/mL, GE Healthcare) was injected intravenously at a flow rate of 3.0 mL/s using a high-pressure syringe (Medrad Stellant CT Injector System, Medrad Inc.). Imaging was obtained with a post-injection delay of 30 s and 70 s after initiation of contrast material injection, corresponding to the arterial and venous phases, respectively. The CT scanning parameters were tube voltage 120 kV, tube current 250–350 mA, slice thickness 5 mm, slice interval 5 mm, field of view 35–50 cm, matrix 512 × 512, rotation time 0.7 s, and pitch 1.375.

The mean interval between CT examination and surgery was 5 days (range, 1–10 days).

CT radiomics feature extraction

Lesion outlining and feature extraction on CT images were performed using Imaging Biomarker Explorer (IBEX) software [25]. Our study focused on the venous images due to the better differentiation of tumor tissue from adjacent normal gastric wall [26]. The arterial images were also analyzed following the same procedure, shown in Supplementary materials. The gastric cancer lesions were manually recognized by a radiologist (S.L., with 6 years' experience in abdominal imaging) and confirmed by another abdominal radiologist (Z.Y.Z., with 12 years' experience in abdominal imaging), who were both blinded to the clinic-pathological information of patients. Focal thickening of the gastric wall by 6 mm or greater with obvious enhancement was defined as the gastric cancer lesion [27]. Each region of interest (ROI) was manually drawn along the margin of the lesion on the largest slice (Fig. 2). The gastric lumen and artifacts were carefully

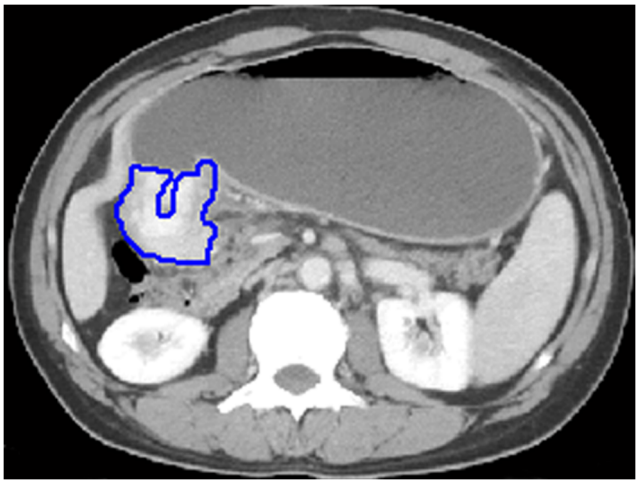

Fig. 2 A 45-year-old man with moderately differentiated gastric adenocarcinoma. During surgery, peritoneal tumor implants were identified and pathologically demonstrated to be peritoneal carcinomatosis. A palliative surgery (bypass gastrojejunostomy) was performed in order to relieve pyloric obstruction. Venous CT image shows a thickened wall with remarkable enhancement in the antrum of the stomach. The blue outline shows an example of the drawn region of interest (ROI) covering the largest image slice of the primary lesion

avoided. A total of 539 quantified features were extracted automatically from the delineated ROIs with seven categories of radiomics features. The detailed explanations and formulas of radiomics features were shown in Supplementary materials, as described previously [28].

Additionally, another abdominal radiologist (J.H., with 9 years' experience in abdominal imaging) performed ROI drawing and feature extractions independently to evaluate the inter-observer variability of radiomics features in gastric cancers.

Feature selections

Feature selections were performed using R software version 3.4.4 (R Foundation for Statistical Computing).

Feature selection was performed first on the basis of reproducibility and redundancy as reported previously [20]. Based on all cases, the intra-class correlation coefficient (ICC) was calculated to evaluate the inter-observer variability of radiomics features extraction using "irr" package (vers. 0.84). Radiomics features with ICC value no lower than 0.8 were regarded as highly reproducible features and were maintained. This resulted in the 498 most stable features being initially included.

Second, redundancy was assessed by pairwise correlation analysis using "caret" package (ver. 6.0–80). The inter-feature correlation coefficient matrix and the absolute correlation coefficient (ACC, mean absolute correlation of a variable with the remaining features) among the above selected features were calculated. Highly correlated features (inter-feature correlation coefficient ≥ 0.80) were found, and the variable with the largest ACC value was removed. Based on the above methods, 52 radiomics parameters were selected for further processing of the study (Supplementary Table 3).

Multivariate model construction

To validate the predictive model, the patients were randomized into two cohorts with a 7 to 3 ratio: 158 for training (124 without PM, 34 with PM) and 75 for testing (64 without PM, 11 with PM). Radiomics features with statistically significant difference in univariate analysis ($p < 0.05$) were entered into a multivariate logistic regression analysis in the primary cohort. Backward stepwise selection was applied based on the Akaike information criterion (AIC) using "MASS" package (ver. 7.3-50). The AIC value and the Hosmer-Lemeshow test were used as the measure of goodness of fit.

The established model was applied to the validation cohort, and the diagnostic performance was assessed with receiver operating characteristic (ROC) analysis.

After feature selections, the support vector machine (SVM) model with a radial basis function kernel was also performed by repeated tenfold cross-validation (CV) with 100 trials. The diagnostic value of CT radiomics analysis in preoperatively predicting the occult PM of AGCs was evaluated and validated further.

In addition, another model including the significant clinicpathological features (major location, CT-based T stage, biopsy pathological type, and differentiation degree in Table 1) was also developed in all cohorts using multivariate logistic regression analysis.

Statistical analyses

The differences of continuous variables were analyzed by the Mann-Whitney *U* test, and the differences of categorical variables were analyzed by chi-square test or Fisher's exact test (count less than 5). The diagnostic performance of CT radiomics features or multivariate models was evaluated using ROC analysis and area under the ROC curve (AUC). Diagnostic sensitivity, specificity, accuracy, positive likelihood ratio, and negative likelihood ratio were also calculated. The diagnostic efficacy of two models was compared using the comparison of ROC curves. All these statistical analyses were performed with SPSS 22.0 or MedCalc 15.2.2. A two-tailed *p* value less than 0.05 was considered statistically significant.

Results

Patient characteristics

There was a significant difference between existing occult PM and no PM in the lesion location, CT-based T stage, biopsy

pathological type, and differentiation degree ($p = < 0.001$–0.019) (Table 1). No significant difference was found between gastric cancers with and without occult PM with regard to the sex, age, and CT-based N stage.

Additionally, there was no significant difference in the clinic-pathological or radiomics features between the primary and validation cohort.

The inter-observer variability and univariate analysis of radiomics features

The inter-observer agreement of seven categories of radiomics features was summarized in Supplementary Table 2.

Six radiomics features including the ID_Energy, LoG(0.5)_Energy, Compactness2, Max Diameter, Orientation, and Surface Area Density differed significantly between gastric cancers with and without occult PM in the primary cohort (Table 2). There were also significant differences between gastric cancers with and without occult PM in the ID_Energy and Surface Area Density in the validation cohort.

ROC analysis showed that the above six features performed well in distinguishing gastric cancers with PM from those without PM in the primary cohort (AUC = 0.618–0.658) (Table 3).

Multivariate models and classifiers for predicting peritoneal metastasis

Compactness2, Max Diameter, and Orientation finally were included into a multivariate logistic regression model in the primary cohort. The Hosmer-Lemeshow test showed an eligible goodness of fit for the model ($p = 0.458$).

The diagnostic performance of the multivariate model in the primary and validation cohorts is shown in Table 4. The diagnostic efficacy of the radiomics model in the validation cohort was slightly worse than that in the primary cohort (AUC, 0.618 vs. 0.741; sensitivity, 0.818 vs. 0.912; specificity, 0.500 vs. 0.508; accuracy, 0.547 vs. 0.595, respectively). The predictive performance of SVM classifications in 100 cross-validation trials was averaged and shown in Supplementary Table 6.

Multivariate logistic analysis showed CT-based T stage as an independent predictive factor of occult PM ($p < 0.001$), seen in Supplementary Table 7. The clinic-pathological model showed slightly better diagnostic efficacy than the radiomics model (AUC, 0.762 vs. 0.724; sensitivity, 0.914 vs. 0.911; specificity, 0.581 vs. 0.495; accuracy, 0.645 vs. 0.575, respectively) (Table 5). However, the comparison of ROC curves showed that the difference of the diagnostic efficacy of the two models was not significant ($p = 0.871$). The goodness of fit of the clinic-pathological and radiomics models was similar (AIC, 157.6 vs. 157.2, respectively).

Discussion

In our cohort, 45/233 (19.3%) had biopsy-confirmed occult PM. For the preoperative clinic-pathological features, our data showed that the lesion location, CT-based T stage, histological type, and differentiation degree significantly differed between AGCs with and without occult PM. Only CT-based T stage was an independent predictive factor of occult PM and other features such as lesion location and biopsy histology may hold some potential in predicting occult PM, yet less effectively compared with CT-based T stage (seen in Supplementary

Table 2 Statistical description and univariate analysis of the selected radiomics signature in gastric cancers with and without PM in the primary cohort (a) and in the validated cohort (b)

	Without PM	With PM	*p* value
(a)			
ID_Energy[a]	12.51 (8.67–17.69)	15.19 (12.05–20.24)	0.013
LoG(0.5)_Energy[b]	5.60 (3.27–10.58)	7.76 (5.00–16.30)	0.036
Compactness2	0.35 (0.25–0.46)	0.44 (0.26–0.63)	0.031
Max Diameter	5.04 (4.12–6.25)	5.58 (5.13–6.81)	0.018
Orientation	15.78 (−12.03–58.55)	− 1.84 (−48.14–35.15)	0.012
Surface Area Density	4.50 (3.83–5.27)	3.93 (3.39–4.58)	0.005
(b)			
ID_Energy[a]	12.23 (8.23–16.23)	15.84 (14.77–24)	0.004
LoG(0.5)_Energy[b]	5.68 (3.56–10.16)	7.47 (3.67–16.57)	0.427
Compactness2	0.33 (0.23–0.44)	0.42 (0.34–0.56)	0.116
Max Diameter	4.93 (4.16–6.33)	5.87 (4.55–7.2)	0.065
Orientation	8.33 (−49.76–64.36)	17.96 (−55.81–63.12)	0.917
Surface Area Density	4.64 (3.9–5.25)	3.92 (3.64–4.07)	0.005

The data are presented as median with interquartile range (1st quartile, 3rd quartile); *PM*, peritoneal metastasis; [a] $\times 10^8$; [b] $\times 10^5$

Table 3 The diagnostic performance of CT radiomics parameters in predicting gastric cancer peritoneal metastasis in the primary cohort (a) and in the validated cohort (b)

Parameter	Cutoff	AUC	Sen	Spe	Acc	+LR	−LR	*p* value
(a)								
ID_Energy	10.65[a]	0.639	0.912	0.427	0.532	1.59	0.21	0.003
LoG(0.5)_Energy	5.82[b]	0.618	0.735	0.532	0.576	1.57	0.50	0.035
Compactness2	0.42	0.621	0.588	0.669	0.652	1.78	0.62	0.038
Max Diameter	5.08	0.632	0.794	0.516	0.576	1.64	0.40	0.008
Orientation	0.46	0.641	0.559	0.669	0.645	1.69	0.66	0.005
Surface Area Density	4.12	0.658	0.647	0.645	0.645	1.82	0.55	0.002
(b)								
ID_Energy	13.14[a]	0.774	1	0.578	0.640	2.37	0	< 0.001
LoG(0.5)_Energy	15.97[b]	0.575	0.364	0.906	0.827	3.87	0.70	0.461
Compactness2	0.40	0.649	0.636	0.703	0.693	2.14	0.52	0.072
Max Diameter	5.41	0.675	0.727	0.625	0.640	1.94	0.44	0.033
Orientation	70.13	0.510	1	0.172	0.293	1.21	0	0.910
Surface Area Density	4.61	0.764	1	0.531	0.600	2.13	0	< 0.001

AUC, area under the receiver operating characteristic curve; *Sen*, sensitivity; *Spe*, specificity; *Acc*, accuracy; *+LR*, positive likelihood ratio; *−LR*, negative likelihood ratio; [a] $\times 10^8$; [b] $\times 10^5$

materials). For CT radiomics analysis, six identified venous features demonstrated a significant difference between AGCs with and without occult PM in the primary cohort. Our data suggested that the larger lesion size and greater heterogeneous gray-level distribution (higher Max Diameter and Energy) indicated a high risk of occult PM in AGCs. Besides, one shape feature of Surface Area Density is relevant to the PM status of AGCs, yet with a relatively low predictive power.

Meanwhile, two multivariate models based on radiomics and clinic-pathological features respectively were built to aid in preoperatively predicting occult PM of AGCs. The radiomics model, a multivariate logistic regression model enrolling Compactness2, Max Diameter, and Orientation, had a higher AUC value of 0.741 than six radiomics features differing significantly between gastric cancers with and without occult PM in the primary cohort. The multivariate model improved the predictive value of radiomics features in PM risk stratification of AGCs. However, the diagnostic performance was slightly worse in the validation cohort than that in the primary cohort. The cross-validation trails based on SVM classifiers also showed similar and mildly reduced predictive value in the validated cohort compared with the primary cohort. Although the radiomics model showed slightly worse diagnostic efficacy than the clinic-pathological model including four traditional clinic-pathological features (Major location, CT-based T stage, biopsy pathological type, and differentiation degree), no significant difference was found between them when comparing ROC curves.

The prevalence of PM varies across studies (9.9–25.6%) [7–10]. This might be related to the exclusion of patients with overt PM, who are not referred for surgery.

Many studies have focused on evaluating the PM status in gastric cancers [6–10, 29, 30]. CT is the most common tool for detecting PM, but its diagnostic performance varies substantially among previously reported studies and its overall sensitivity is poor (0.33, 95% CI, 0.16–0.56) [14]. Kim et al, comparing CT-based true-negatives and false-negatives, reported that there was a significant difference in histologic type, tumor

Table 4 The diagnostic performance of multivariate model in predicting peritoneal metastasis in primary and validation cohorts

	AUC	Sen	Spe	Acc	+LR	−LR	*p* value
Primary cohort	0.741	0.912	0.508	0.595	1.85	0.17	< 0.001
Validation cohort	0.618	0.818	0.500	0.547	1.64	0.36	0.1501

AUC, area under the receiver operating characteristic curve; *Sen*, sensitivity; *Spe*, specificity; *Acc*, accuracy; *+LR*, positive likelihood ratio; *−LR*, negative likelihood ratio

Table 5 The comparison of two multivariate models for predicting gastric cancer peritoneal metastasis

	Clinic-pathological model	Radiomics model
Variables	CT-based T stage	Compactness2
	Major location	Max Diameter
	Differentiation degree	Orientation
	Differentiation type	
AUC	0.762	0.724
Sensitivity	0.914	0.911
Specificity	0.581	0.495
Accuracy	0.645	0.575
AIC	157.6	157.2
p value	0.871	

AUC, area under the receiver operating characteristic curve; *AIC*, the Akaike information criterion

size, T stage, and N stage [8]. In another study of 640 cases, four CT-based features (depth of invasion, lymph node metastasis status, tumor size, and tumor thickness) were significantly correlated with the PM status, which is partly consistent with our findings [10].

CT radiomics analysis, a quantitative and non-invasive tool, attracts increasing attention for the preoperative prediction of occult PM of gastric cancers. Dong et al reported that venous CT radiomics analysis combining both primary tumor and nearby peritoneum had an excellent prediction value of occult PM of AGCs [24]. In another study, Kim et al found that CT texture features over the omentum, especially entropy, held potential promise in distinguishing gastric cancers with and without occult PM, indicating that CT texture analysis over the omentum might be a useful adjunct for the prediction of occult PM in AGCs [21]. Nevertheless, outlining ROIs over the omentum in only one cross-sectional slice shows the difficulty in ensuring repeatability and robustness. It is also unavailable in emaciated patients lacking identifiable omentum. Anyhow, CT texture analysis over the omentum still deserves further investigation.

Our study had limitations. First, CT images were retrospectively obtained from several scanners, and acquisition parameters varied, which might influence the extracted features. Nevertheless, a good inter-scanner agreement of the CT texture analysis was confirmed when using different scanners with different vendors and acquisition processes [31]. Second, the largest slice of the lesion, rather than the whole lesion or the area of greatest enhancement, was selected for radiomics analysis. The whole-lesion analysis might be more representative for the heterogeneous characteristics of the lesions. However, the comparison of single-level and whole-tumor CT texture analyses of single lesions showed fairly comparable results in previous studies [31, 32]. Moreover, outlining the area of greatest enhancement as the ROIs might decrease the effect of necrotic tissues and reflect angiogenesis more intensely, but there might exist site-by-site biases when placing ROIs [33, 34]. Therefore, the ROIs outlining the largest slice of the lesion might not only represent the heterogeneity of the whole lesion but also improve the repeatability and reproducibility. Third, we performed radiomics analysis with a focus on venous phase, since features on arterial phase proved poorer in predicting occult PM of AGCs. In our study, early arterial phase images were obtained with a delay time of 30 s. We speculated that different delay time of arterial phase (from 30 to 45 s) may influence radiomics features and its diagnostic performance, which required further investigation. Fourth, only axial images were used for radiomics analysis, but some gastric cancers are better seen on coronal or sagittal views [27]. Coronal and sagittal images by multi-planar reconstruction were unavailable in most cases of our retrospective cohort. Radiomics sub-analysis on available coronal and sagittal images is shown in Supplementary materials. Finally, peritoneal cytology was not used routinely in our study (seen in Supplementary materials). Positive peritoneal cytology is considered as an important prognostic factor for gastric cancers and has an impact in selecting therapeutic strategy [35]. However, the detecting methods of peritoneal cytology still lack a consensus and gold standard. The role of radiomics analysis in predicting gastric cancers with positive peritoneal cytology deserves to be investigated further.

In conclusion, a venous CT radiomics model derived from the primary tumor was developed. It showed a good diagnostic value and fitted performance in predicting occult PM of AGCs. CT radiomics analysis holds potential value in preoperatively identifying AGCs with suspicious PM, who should undergo further exploratory laparoscopy for definite diagnosis.

Funding This study has received funding by the National Natural Science Foundation of China (ID: 81501441, 81601463, 81871410), Social Development Foundation of Jiangsu Province (BE2015605), Natural Science Foundation of Jiangsu Province (ID: BK20150109), Jiangsu Province Health and Family Planning Commission Youth Scientific Research Project (ID: Q201508), Six Talent Peaks Project of Jiangsu Province (ID: 2015-WSN-079), and Jiangsu Provincial Medical Youth Talent (ID: QNRC2016040).

Compliance with ethical standards

Guarantor The scientific guarantor of this publication is Zhengyang Zhou, MD.

Conflict of interest The authors of this manuscript declare no relationships with any companies, whose products or services may be related to the subject matter of the article.

Statistics and biometry No complex statistical methods were necessary for this paper.

Informed consent Written informed consent was waived by the Institutional Review Board.

Ethical approval Institutional Review Board approval was obtained.

Methodology
- retrospective
- diagnostic or prognostic study
- performed at one institution

References

1. Fitzmaurice C, Allen C, Barber RM et al (2017) Global, regional, and national cancer incidence, mortality, years of life lost, years lived with disability, and disability-adjusted life-years for 32 cancer groups, 1990 to 2015: a systematic analysis for the global burden of disease study. JAMA Oncol 3:524–548
2. Thomassen I, van Gestel YR, van Ramshorst B et al (2014) Peritoneal carcinomatosis of gastric origin: a population-based study on incidence, survival and risk factors. Int J Cancer 134: 622–628

3. Abbasi SY, Taani HE, Saad A, Badheeb A, Addasi A (2011) Advanced gastric cancer in Jordan from 2004 to 2008: a study of epidemiology and outcomes. Gastrointest Cancer Res 4:122–127
4. Wallace MB, Nietert PJ, Earle C et al (2002) An analysis of multiple staging management strategies for carcinoma of the esophagus: computed tomography, endoscopic ultrasound, positron emission tomography, and thoracoscopy/laparoscopy. Ann Thorac Surg 74: 1026–1032
5. Li K, Cannon JGD, Jiang SY et al (2018) Diagnostic staging laparoscopy in gastric cancer treatment: a cost-effectiveness analysis. J Surg Oncol 117:1288–1296
6. Chang DK, Kim JW, Kim BK et al (2005) Clinical significance of CT-defined minimal ascites in patients with gastric cancer. World J Gastroenterol 11:6587–6592
7. Gretschel S, Siegel R, Estévez-Schwarz L, Hünerbein M, Schneider U, Schlag PM (2006) Surgical strategies for gastric cancer with synchronous peritoneal carcinomatosis. Br J Surg 93:1530–1535
8. Kim SJ, Kim HH, Kim YH et al (2009) Peritoneal metastasis: detection with 16- or 64-detector row CT in patients undergoing surgery for gastric cancer. Radiology 253:407–415
9. Yajima K, Kanda T, Ohashi M et al (2006) Clinical and diagnostic significance of preoperative computed tomography findings of ascites in patients with advanced gastric cancer. Am J Surg 192:185–190
10. Yan C, Zhu ZG, Yan M et al (2010) Value of multidetector-row CT in the preoperative prediction of peritoneal metastasis from gastric cancer: a single-center and large-scale study. Zhonghua Wei Chang Wai Ke Za Zhi 13:106–110
11. Fujii S, Matsusue E, Kanasaki Y et al (2008) Detection of peritoneal dissemination in gynecological malignancy: evaluation by diffusion-weighted MR imaging. Eur Radiol 18:18–23
12. Bozkurt M, Doganay S, Kantarci M et al (2011) Comparison of peritoneal tumor imaging using conventional MR imaging and diffusion-weighted MR imaging with different b values. Eur J Radiol 80:224–228
13. Fehniger J, Thomas S, Lengyel E et al (2016) A prospective study evaluating diffusion weighted magnetic resonance imaging (DW-MRI) in the detection of peritoneal carcinomatosis in suspected gynecologic malignancies. Gynecol Oncol 142:169–175
14. Wang Z, Chen JQ (2011) Imaging in assessing hepatic and peritoneal metastases of gastric cancer: a systematic review. BMC Gastroenterol 11:19
15. Giganti F, Antunes S, Salerno A et al (2017) Gastric cancer: texture analysis from multidetector computed tomography as a potential preoperative prognostic biomarker. Eur Radiol 27:1831–1839
16. Giganti F, Marra P, Ambrosi A et al (2017) Pre-treatment MDCT-based texture analysis for therapy response prediction in gastric cancer: comparison with tumour regression grade at final histology. Eur J Radiol 90:129–137
17. Liu S, Liu S, Ji C et al (2017) Application of CT texture analysis in predicting histopathological characteristics of gastric cancers. Eur Radiol 27:4951–4959
18. Liu S, Shi H, Ji C et al (2018) Preoperative CT texture analysis of gastric cancer: correlations with postoperative TNM staging. Clin Radiol 73:756.e751–756.e759
19. Ma Z, Fang M, Huang Y et al (2017) CT-based radiomics signature for differentiating Borrmann type IV gastric cancer from primary gastric lymphoma. Eur J Radiol 91:142–147
20. Hou Z, Yang Y, Li S et al (2018) Radiomic analysis using contrast-enhanced CT: predict treatment response to pulsed low dose rate radiotherapy in gastric carcinoma with abdominal cavity metastasis. Quant Imaging Med Surg 8:410–420
21. Kim HY, Kim YH, Yun G, Chang W, Lee YJ, Kim B (2018) Could texture features from preoperative CT image be used for predicting occult peritoneal carcinomatosis in patients with advanced gastric cancer? PLoS One 13:e0194755
22. Burbidge S, Mahady K, Naik K (2013) The role of CT and staging laparoscopy in the staging of gastric cancer. Clin Radiol 68:251–255
23. Power DG, Schattner MA, Gerdes H et al (2009) Endoscopic ultrasound can improve the selection for laparoscopy in patients with localized gastric cancer. J Am Coll Surg 208:173–178
24. Dong D, Tang L, Li ZY et al (2019) Development and validation of an individualized nomogram to identify occult peritoneal metastasis in patients with advanced gastric cancer. Ann Oncol. https://doi.org/10.1093/annonc/mdz001
25. Zhang L, Fried DV, Fave XJ, Hunter LA, Yang J, Court LE (2015) IBEX: an open infrastructure software platform to facilitate collaborative work in radiomics. Med Phys 42:1341–1353
26. Huang YQ, Liang CH, He L et al (2016) Development and validation of a radiomics nomogram for preoperative prediction of lymph node metastasis in colorectal cancer. J Clin Oncol 34:2157–2164
27. Kim HJ, Kim AY, Oh ST et al (2005) Gastric cancer staging at multi-detector row CT gastrography: comparison of transverse and volumetric CT scanning. Radiology 236:879–885
28. Aerts HJ, Velazquez ER, Leijenaar RT et al (2014) Decoding tumour phenotype by noninvasive imaging using a quantitative radiomics approach. Nat Commun 5:4006
29. Nakagawa S, Nashimoto A, Yabusaki H (2007) Role of staging laparoscopy with peritoneal lavage cytology in the treatment of locally advanced gastric cancer. Gastric Cancer 10:29–34
30. Li Z, Li Z, Zhang L et al (2018) Staging laparoscopy for locally advanced gastric cancer in Chinese patients: a multicenter prospective registry study. BMC Cancer 18:63
31. Ahn SJ, Kim JH, Park SJ, Han JK (2016) Prediction of the therapeutic response after FOLFOX and FOLFIRI treatment for patients with liver metastasis from colorectal cancer using computerized CT texture analysis. Eur J Radiol 85:1867–1874
32. Ng F, Kozarski R, Ganeshan B, Goh V (2013) Assessment of tumor heterogeneity by CT texture analysis: can the largest cross-sectional area be used as an alternative to whole tumor analysis? Eur J Radiol 82:342–348
33. Lubner MG, Stabo N, Lubner SJ et al (2015) CT textural analysis of hepatic metastatic colorectal cancer: pre-treatment tumor heterogeneity correlates with pathology and clinical outcomes. Abdom Imaging 40:2331–2337
34. Komori M, Asayama Y, Fujita N et al (2013) Extent of arterial tumor enhancement measured with preoperative MDCT gastrography is a prognostic factor in advanced gastric cancer after curative resection. AJR Am J Roentgenol 201:W253–W261
35. Tustumi F, Bernardo WM, Dias AR et al (2016) Detection value of free cancer cells in peritoneal washing in gastric cancer: a systematic review and meta-analysis. Clinics (Sao Paulo) 71:733–745